

COMITATO NAZIONALE PER L'ENERGIA NUCLEARE
Laboratori Nazionali di Frascati

LNF-71/16
3 Maggio 1971

C. Bacci, R. Baldini-Celio, G. Capon, C. Mencuccini, G. P. Murtas,
G. Penso, A. Reale, G. Salvini and M. Spinetti : EXPERIMENTAL
TEST OF QUANTUM ELECTRODYNAMICS BY 2γ ANNIHILATION
AT 1.4-2.4 GeV TOTAL ENERGY WITH THE e^+e^- STORAGE RING
ADONE.

Laboratori Nazionali di Frascati del CNEN
Servizio Documentazione

LNF - 71/16
3 Maggio 1971

C. Bacci^(x), R. Baldini-Celio, G. Capon, C. Mencuccini, G. P. Mur^{ta}s, G. Penso^(x), A. Reale, G. Salvini^(x) and M. Spinetti: EXPERIMENTAL TEST OF QUANTUM ELECTRODYNAMICS BY 2γ ANNIHILATION AT 1.4 - 2.4 GeV TOTAL ENERGY WITH THE e^+e^- STORAGE RING ADONE.

We report our preliminary results on the reaction



observed at the 2×1.5 GeV "Adone" storage ring of the Frascati laboratories.

This reaction has been studied for values of E , the single beam energy, ranging from 0.7 to 1.2 GeV and for values of θ (the angle of emission of the photons with respect to the beam directions) lying in the two intervals $20^\circ - 45^\circ$ and $70^\circ - 110^\circ$.

The aim of the experiment was to test the validity of quantum electrodynamics (QED) for a space-like electron propagator, at high momentum transfers, up to a maximum value of 1.6 GeV. On basis of the present analysis of 399 annihilation events, which covers only a part of our total film, we have found that our results do not exhibit any evident discrepancy from QED, within our statistical and systematic errors.

Reaction (1) is a pure electromagnetic process and allows a very clear test of QED. The reaction is described at lowest order by the graphs of Fig. 1.

The square four momentum of the virtual electron is respectively given by:

(x) - Istituto di Fisica dell'Università di Roma, and Istituto Nazionale di Fisica Nucleare - Sezione di Roma.

2.

$$q_1^2 = 4E^2 \sin^2(\theta/2) \quad \text{for graph (a)}$$

$$q_2^2 = 4E^2 \cos^2(\theta/2) \quad \text{for graph (b).}$$

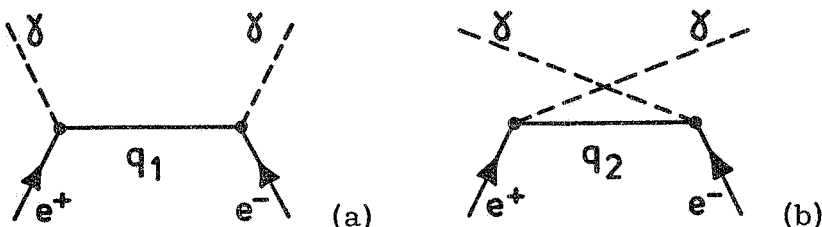


FIG. 1 - Feynman graphs contributing to the process (1), in the first order approximation.

According to pure QED the differential cross section is given by⁽¹⁾:

$$(2) \quad \frac{d\sigma}{d \cos \theta} = \pi r_o^2 \left(\frac{m}{E} \right)^2 \frac{2 - \sin^2 \theta}{2 \sin^2 \theta}$$

where m is the electron mass and r_o is the electron classical radius.

In contrast to reactions which proceed through the annihilation channel, the reaction we observe exhibits an angular dependence of the momentum transfers q_1, q_2 .

At small angles (where $q_1 \approx E\theta$) the contribution to the cross section of the graph (a) (Fig. 1) with low momentum transfer q_1 , greatly dominates that of graph (b), while at 90° (where $q_1 = q_2 = E\sqrt{2}$) both graphs give equal contributions. Therefore an eventual deviation from pure QED at high momentum transfer may be detected by measuring the angular distribution of reaction (1), or the ratio of the cross section around $\theta = 90^\circ$ to that at small values of θ .

We emphasize that in this procedure the knowledge of the absolute luminosity of the e^+e^- machine is not necessary, since the verification of QED only involves the ratio of the cross section at different angles.

The experimental apparatus is schematically shown in Fig. 2. It consists of four similar γ -ray telescopes: T_1, T_1' centered around $\theta = 30^\circ$ and T_2, T_2' centered around $\theta = 90^\circ$; each telescope is composed of four scintillation counters $S_0 - S_3$ (the first one being in anticoincidence), three lead converters, and eight bigap optical spark chambers. The total solid angle of the four telescopes is 3 steradians. A photon is detected in one of the telescopes whenever, by conversion and electromagnetic multiplica-

tion, it gives a coincidence $\overline{S_0} \cdot ((S_1 \cdot S_2) + (S_2 \cdot S_3))$ between the counters (Fig. 2). A $\gamma\gamma$ annihilation event is defined by a coincidence $(T_1 \cdot T_1') + (T_2 \cdot T_2')$ between the telescopes. The total useful conversion thickness in each telescope is 3.5 RL and the corresponding photon detection efficiency, which is the same for small and large angle telescopes, has been experimentally measured and also checked by a Montecarlo calculation⁽²⁾. This photon detection efficiency varies from 0.80 to 0.85 for photon energies varying from 700 to 1200 MeV. The direction of a photon is measured in the spark chambers with a precision of about $\pm 2^\circ$.

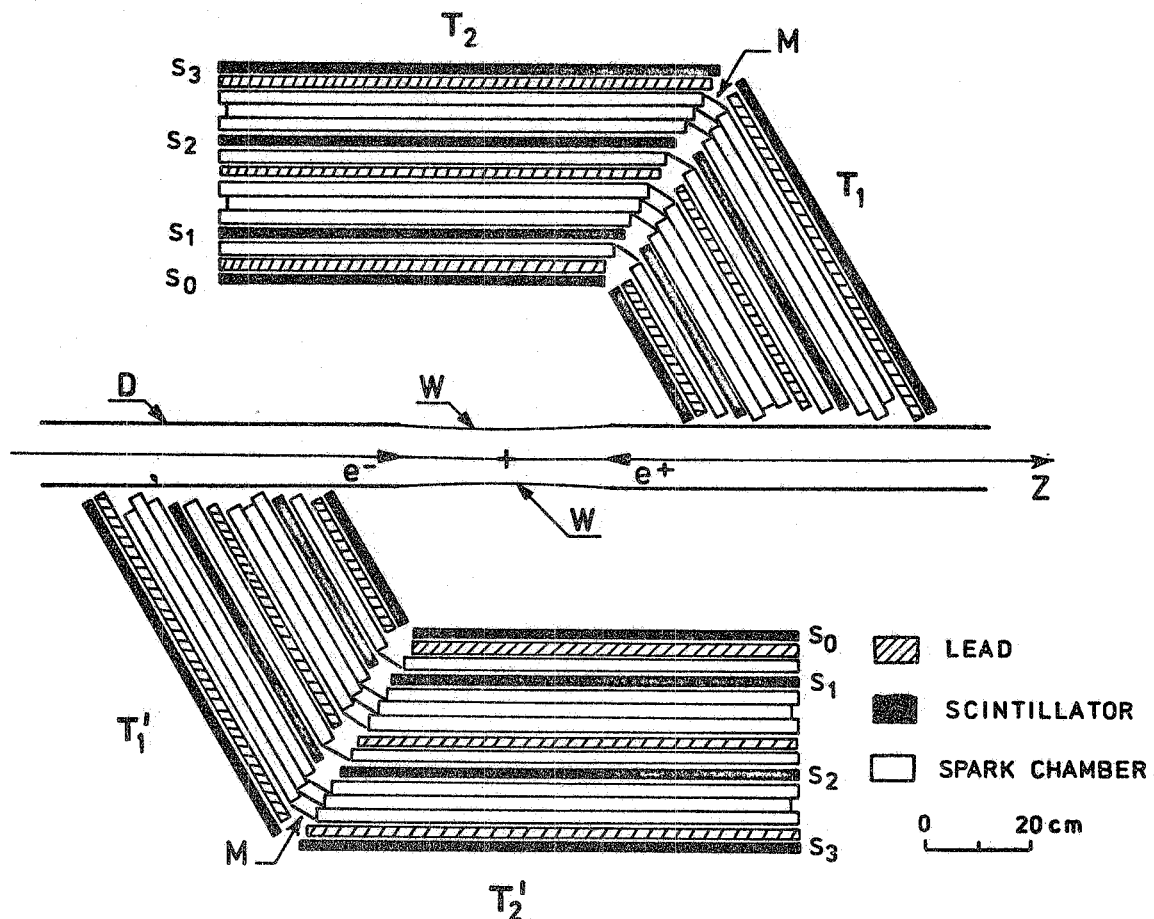


FIG. 2 - Experimental apparatus : Front view seen from Adone center; D: Adone doughnut; W: 0.15 mm stainless steel window. The side view of the T_1 (T_1') spark chamber is seen through the T_2 (T_2') spark chambers, by mean of the small mirrors M.

Anticoincidence counters (S_0) in front of the telescopes reject charged particles and cosmic rays. In the worst conditions the counting loss from anticoincidence accidentals due to machine background is less than 1.5 %.

The spark chambers are photographed with 90° stereoscopy from Adone center (front view) and along the beam line (side

4.

view). In the pictures, $\gamma\gamma$ annihilation events are easily distinguished from machine background or cosmic rays. A typical photograph is shown in Fig. 3.

The measurements on the photographs give the angles θ_{p_1} , θ_{p_2} (θ_p being the projection of θ on a vertical plane containing the beams) and ψ_1 , ψ_2 (azimuthal angle) of the two photons, as well as the abscissa Z of the interaction point along the beam direction. The values of Z are spread around the center ($Z = 0$) of the straight section since the interaction points have a Gaussian distribution with a R. M. S. width of about 20 cm. The transverse dimensions of the beams are about 1 mm in the radial direction and about 0.01 mm in the vertical direction.

Among the scanned events we have selected those which satisfy the following conditions :

- a) $|Z| \leq 7.5$ cm. This is the target region which is seen with full geometrical efficiency from all the four telescopes.
- b) $|\theta_{p_1} - \theta_{p_2}| \leq 5^\circ$, $|\psi_1 - \psi_2| \leq 10^\circ$. These conditions define "collinear" photons in the apparatus.

The experimental results are shown in Table I :

- In column 1 we report all the energies (E) at which measurement were taken. Because of the low statistics, we have grouped the data in four energy intervals. \bar{E} (column 2) is the mean energy of each interval weighted by the luminosity.
- N_1 and N_2 (columns 3 and 4) are the number of $\gamma\gamma$ annihilation events detected at small angles (telescopes T_1 , T'_1) and at large angles (telescopes T_2 , T'_2) respectively.
- N_1^c and N_2^c (columns 5 and 6) are the same numbers corrected for photon conversion in materials preceding the anticoincidence (about + 5 %) and radiative corrections (+ 8 % for N_1 and + 12 % for N_2). These last corrections have been evaluated according to the formula of Tsai⁽³⁾.
- R^{exp} (column 7) is the ratio N_1^c/N_2^c .
- $R^{\text{QED}} = \epsilon_1^{\text{QED}}/\epsilon_2^{\text{QED}}$ (column 8) is the corresponding value predicted by QED. ϵ_1^{QED} and ϵ_2^{QED} have been calculated by integrating the cross section (2) over the solid angle of the telescopes (T_1 , T'_1) and (T_2 , T'_2) respectively. The length of the interaction region and the photon detection efficiency have been taken into account.
- L (column 9) is the time-integrated luminosity. L has been obtained by multiplying by a normalization factor the luminosity values measured in a different Adone straight section by the small angle e^+e^- elastic scattering monitor of the Frascati-Rome-Padova group⁽⁴⁾.

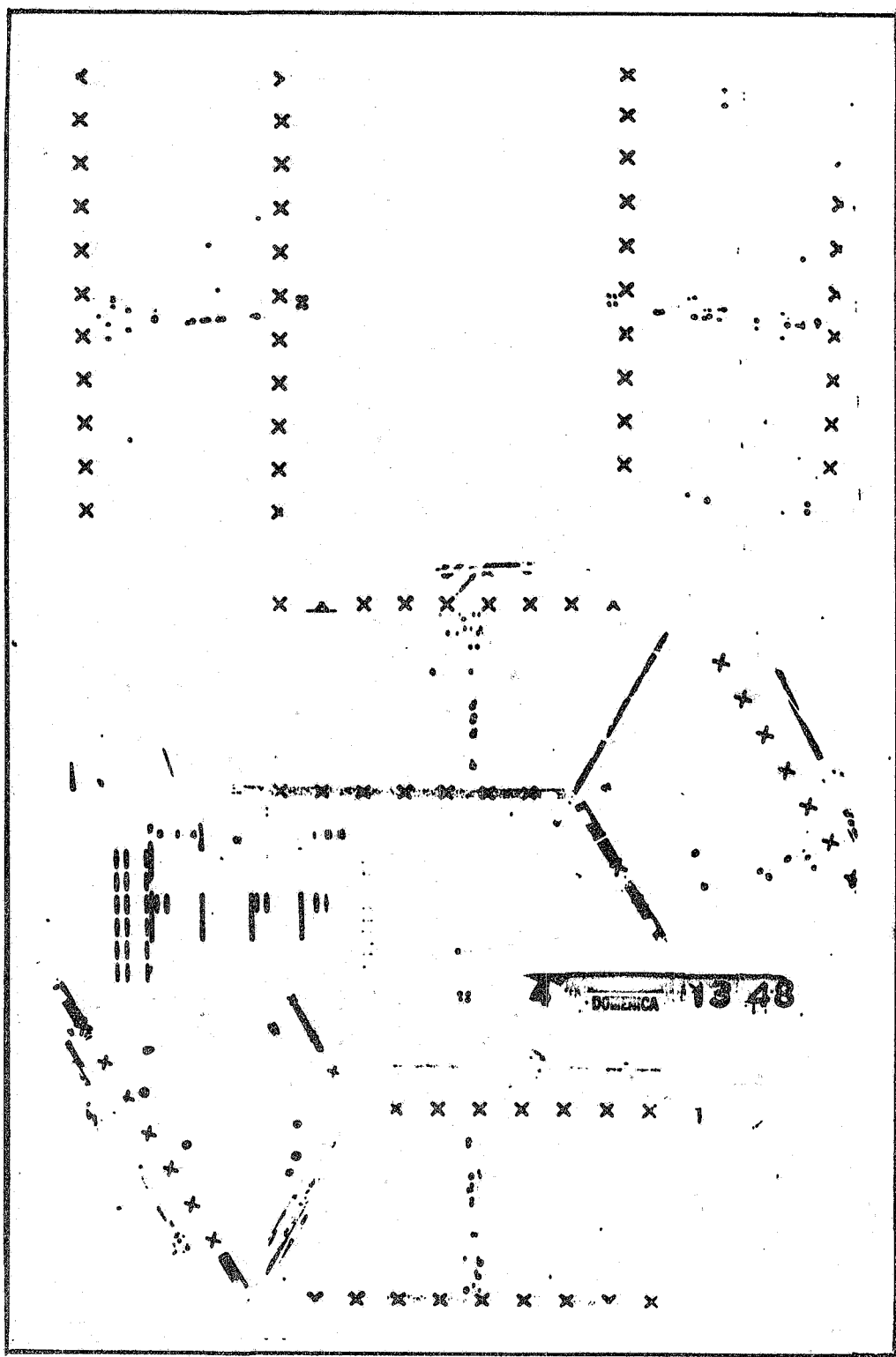


FIG. 3 - Picture of a $\gamma\gamma$ annihilation event; each photograph contains in the lower part the front view and in the upper part the side views.

TABLE I

Experimental results for the process $e^+ + e^- \rightarrow \gamma + \gamma$.

(1)	(2)	(3)	(4)	(5)	(6)	(7)	(8)	(9)
E (MeV)	\bar{E} (MeV)	N_1	N_2	N_1^C	N_2^C	R^{exp}	R^{QED}	L (10^{32} cm^{-2})
700		25	3					40
750		31	13					76
800		2	2					16
825		16	8					70
	770	74		26	83, 1	30, 0	2.77 ± 0.63	2, 98
850		18	5					62
875		17	9					92
900		15	6	27, 5	81, 8	31, 6	2.59 ± 0.58	2, 98
925 ^x		24	7, 5					99
	893	74						112
925 ^x		24	7, 5					112
950	945	56	21	28, 5	91, 8	33, 1	2.76 ± 0.60	2, 98
		80						112
1000		16	5					404
1050		37	14					151
1100		7	2	25	73, 1	29, 1	2.50 ± 0.54	307
1200		4	4					46
	1067	64						107
		64						611
		TOTAL		292	107	329, 8	123, 8	
								1694

Col. (1) : Energy (E) of each beam.

Col. (2) : Average energy (\bar{E}), weighted by the luminosity L.Col. (3), (4) : Number of $\gamma\gamma$ events collected at small angles (N_1), and at large angles (N_2).

Col. (5), (6) : The same numbers corrected for photon conversion before the anticoincidence and for the radiative corrections.

Col. (7) : Ratio R^{exp} between N_1^C and N_2^C .Col. (8) : The corresponding ratio R^{QED} predicted by pure QED.

Col. (9) : Time-integrated luminosity, measured during the experiment.

(x) - Data collected at E=925 MeV have been splitted into two equal parts in order to have similar statistics for each \bar{E} value.

This normalization factor, which turns out to be 0.92 ± 0.05 , has been evaluated by requiring that the total number N_1^C of our events at small angles, that is, those in the region dominated by the low momentum transfers, agrees with the corresponding QED predictions.

Our verification of QED validity consists mainly in the comparison of the values of R^{exp} and R^{QED} (columns 7, 8). These values are given in Fig. 4 versus the total energy ($2E$) of the e^+e^- beams. As one can see from Fig. 4, the QED predictions are in agreement with the experimental results within one standard deviation.

Eventual systematic errors on the ratio R may originate from the definition of the geometrical acceptance, from slight differences in γ ray detection in the four telescopes, from the angular resolution of the apparatus at small angles where the cross section is steeply decreasing, and from spurious event contamination.

We assume for all these effects a total systematic error of 5%.

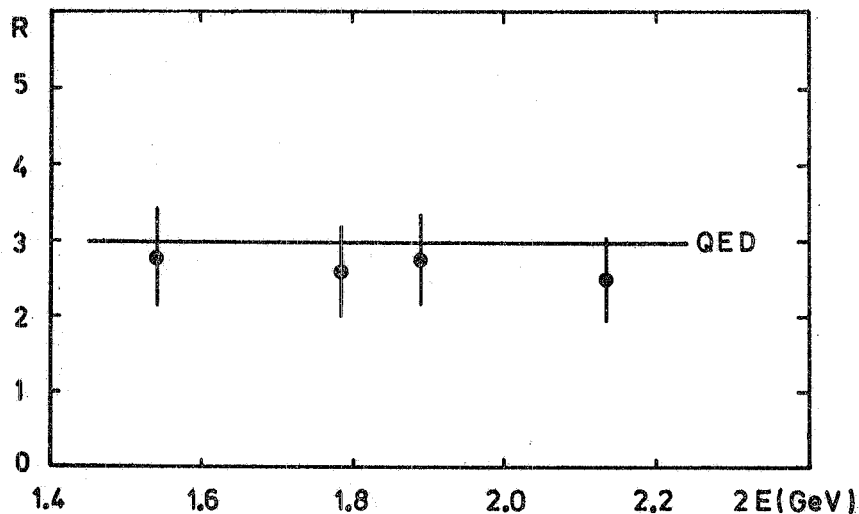


FIG. 4 - Energy behaviour of the ratio $R \stackrel{\text{exp}}{=} N_1^c / N_2^c$ between the events at small angles (telescopes T_1, T'_1) and at large angles (telescopes T_2, T'_2). Full line represents the QED prediction. Errors are statistical only.

In Fig. 5 we give the angular distribution of all our events summed over all energies. The full line is the prediction of QED normalized to our events N_1 at small angles. At large angles the agreement between experimental data and QED prediction is satisfactory within statistics and possible systematic errors.

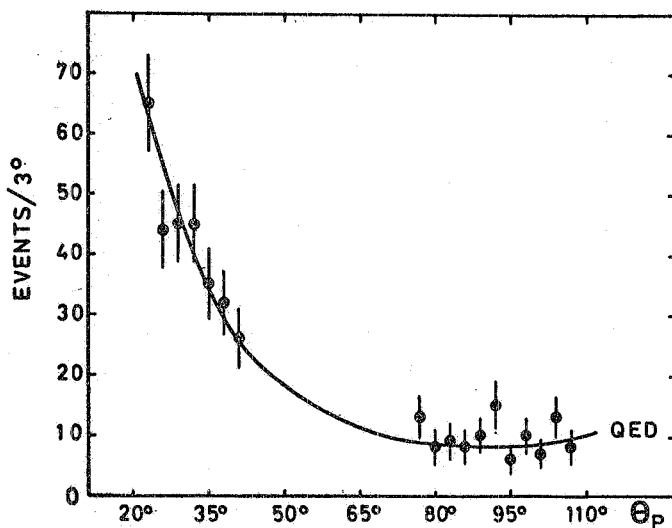


FIG. 5 - Angular distribution of all the events (summed over all energies) versus θ_p . θ_p is the projection of θ on a vertical plane containing the beams. The full line represents the QED prediction, normalized in the region of small angles. Errors are statistical only.

In Fig. 6 we show the ratio between the experimental and the theoretical cross sections versus the momentum transfer q .

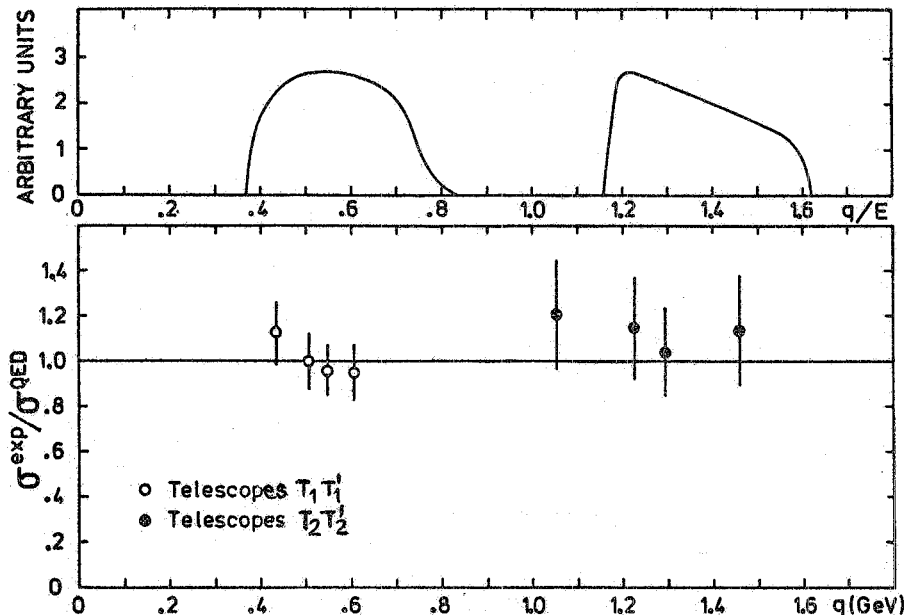


FIG. 6 - Ratio between the experimental and theoretical cross section versus the momentum transfer q . For each pair of telescopes, the four experimental points correspond to the \bar{E} values reported in Table I. For the events in the telescopes T_1, T'_1 , we assume $q=q_1$ because the graph (b) (Fig. 1) gives a negligible contribution at small angles. For the events in telescopes T_2, T'_2 we have $q \approx q_1 \approx q_2$. The average of the experimental points relative to the telescopes T_1, T'_1 is normalized to 1; this follows directly from our definition of the luminosity L . The q/E resolution of our apparatus is shown in the upper part of the figure.

It is customary to express the experimental verification of QED by giving the lower limit for a certain cut off parameter

Since Kroll⁽⁵⁾ has shown that a consistent QED modification for the electron propagator should be of the form of q^4/Λ^4 (q^2 being the square four momentum of the virtual electron) the agreement between theory and experiment is currently measured⁽⁶⁾ using the parametrization :

$$(3) \quad \frac{\sigma_{\text{exp}}}{\sigma_{\text{QED}}} = 1 + \frac{2q^4}{\Lambda_+^4} = (\text{at } \theta=90^\circ) 1 + \frac{8E^4}{\Lambda_+^4} .$$

In this case, assuming that QED theory holds at small angles, we obtain from our experiment :

$$\Lambda_+ \geq 2.0 \text{ GeV} \quad \Lambda_- \geq 2.6 \text{ GeV}$$

with a 95% confidence level, having also included the above mentioned 5% systematic error.

These values may be compared with those obtained by the other experiments⁽⁶⁾ which have tested the electron propagator, and in particular with the value $\Lambda_+ \geq 1.1 \text{ GeV}$ obtained at lower energies by an analogous storage ring experiment of V. E. Balakin et al.^{(7) (x)}.

We would like to thank Prof. C. Pellegrini who participated at the earlier stages of this experiment. Prof. B. Touschek for its interest and useful discussions, the machine staff for continuous collaboration, and the Frascati-Roma-Padova group for giving us their "monitor" data. We are also indebted to our technicians V. Bidoli and to Mr. Di Stefano and co-workers for all their work on the setting up and maintenance of the apparatus.

REFERENCES. -

- (1) - R. Gatto, Proc. Intern. Symp. on Electron and Photon Interactions at High Energies, Hamburg (1965), Vol. I, p. 106.
- (2) - G. Capon, M. A. Locci, G. P. Murtas and G. Penso, Frascati report LNF-70/13 (1970).
- (3) - Y. S. Tsai, Phys. Rev. 137, 730 (1965).
- (4) - G. Barbiellini et al., Atti Accademia Naz. dei Lincei XLIV, 233 (1968); Frascati-Roma-Padova Collaboration, Frascati report LNF-70/38 (1970).
- (5) - N. Kroll, Nuovo Cimento 45A, 65 (1966).
- (6) - R. Wilson, Rapporteur talk at XV Intern. Conf. on High Energy Physics, Kiev (1970).
- (7) - V. E. Balakin et al., Phys. Letters 34B, 99 (1971).

(x) - These authors use a formula slightly different from (3): $\frac{\epsilon_{\text{exp}}}{\epsilon_{\text{QED}}} = 1 + (2E/\Lambda)^4$ and obtain $\Lambda \geq 1.3 \text{ GeV}$ with 95% confidence level. When using expression (3) their lower limit becomes $\Lambda \geq 1.1 \text{ GeV}$.